Insulator-metal transition in $BaCo_{0.9}Ni_{0.1}S_{2-y}Se_y$

J. W. Schweitzer and L. S. Martinson*
Department of Physics and Astronomy, The University of Iowa, Iowa City, Iowa 52242

N. C. Baenziger and D. C. Swenson
Department of Chemistry, The University of Iowa, Iowa City, Iowa 52242

Victor G. Young, Jr.
Department of Chemistry, University of Minnesota, Minneapolis, Minnesota 55455

Ilia Guzei
Department of Chemistry, Iowa State University, Ames, Iowa 50011
(Received 20 April 2000; revised manuscript received 30 June 2000)

Compounds of the Se-doped layered transition-metal sulfide series $BaCo_{0.9}Ni_{0.1}S_{2-y}Se_y$ ($y \leqslant 0.4$) were prepared and structural, magnetic, and electrical properties were investigated. These compounds exhibit the unusual first-order antiferromagnetic semiconductor to paramagnetic metal transition with decreasing temperature that was previously seen in the sulfur-deficient $BaCo_{1-x}Ni_xS_{2-y}$ series. This transition is associated with a major structural change. The previously unknown crystal structure of the low-temperature phase is reported. Electrical resistance and magnetic susceptibility measurements are used to construct the phase diagram for $BaCo_{0.9}Ni_{0.1}S_{2-y}Se_y$. Doping with Se increases the insulator-metal transition temperature, but has very little effect on other properties since it substitutes for S only in the BaS layers.

I. INTRODUCTION

The sulfur-deficient $BaCo_{1-x}Ni_xS_{2-y}$ series[1] exhibits a puzzling first-order insulator to metal transition with decreasing temperature near 200 K for compositions in the range $0.05 \leqslant x,y \leqslant 0.20$. Recently we have found the same transition in the stoichiometric $BaCo_{0.9}Ni_{0.1}S_{2-y}Se_y$ series. This transition is associated with a major crystalline distortion to a structure of lower symmetry. What is remarkable is that these materials exhibit semiconducting, antiferromagnetic behavior at high temperatures, and metallic, Pauli paramagnetic behavior at low temperatures. Thus two common mechanisms for metal-to-insulator transitions with decreasing temperature, namely antiferromagnetic ordering and crystalline structure distortion, are associated with this transition, and yet the transition is from insulator to metal with decreasing temperature. Thus these materials present another challenge to our understanding of metal-insulator transitions. Although the sulfur-deficient series has received considerable attention, the crystal structure of the low-temperature metallic phase had not been fully characterized and in some cases incorrectly described as a very small monoclinic distortion of the high-temperature structure. Since knowing the low-temperature structure is a prerequisite for any serious attempt to understand the physics involved, we have devoted considerable effort to determine this structure. Our previous single-crystal x-ray studies of the sulfur-deficient compounds had identified the fundamental monoclinic unit cell, but had failed to refine satisfactorily the atomic positions owing to complications associated with twinning and superstructures. Fortunately we have been to able to determine the low-temperature structure using single-crystal x-ray diffraction results for the stoichiometric Se-doped compounds. In this paper we will describe this structure, report electrical and magnetic properties for sintered polycrystalline samples, and construct the phase diagram for the $BaCo_{0.9}Ni_{0.1}S_{2-y}Se_y$ system. In addition we discuss some materials issues such as the failure of rapidly quenched samples to exhibit the transition and the importance of proper annealing of samples.

Above the insulator-metal transition temperature the structural, electrical, and magnetic properties of these $BaCo_{0.9}Ni_{0.1}S_{2-y}Se_y$ compounds are qualitatively identical with those of the parent compound $BaCoS_2$. This layered transition-metal sulfide is a semiconductor that exhibits long-range antiferromagnetic order below $T_N = 310$ K.[1] The resistivity above the Néel temperature is characterized by a small thermal activation energy of approximately 0.15 eV. Since the quasi-two-dimensional Co-S layers in the $BaCoS_2$ structure are expected to give rise to antibonding σ^* bands at the Fermi level, it is most probable that $BaCoS_2$ is an antiferromagnetic insulator as the result of strong electron correlations. Indeed, band structure calculations[2,3] for the metallic compound $BaNiS_2$, which is nearly isostructural[4–6] with $BaCoS_2$, predict partially filled $d_{x^2-y^2}$ σ^* bands near the Fermi energy that overlap $d_{z^2-r^2}$ and $d_{xz,yz}$ subbands. Thus $BaCoS_2$ and the series $BaCo_{1-x}Ni_xS_2$ have received considerable attention[7–21] since $BaCoS_2$ is a probable quasi-two-dimensional Mott-Hubbard insulator that exhibits a Mott transition as Ni is substituted for Co.

Initial interest in $BaCoS_2$ was owing to the observation[5] that its structural, magnetic, and electrical properties are quite similar to those of La_2CuO_4, the parent compound of the high-T_C cuprate superconductors. Unfortunately it has not been possible to create a superconducting phase by doping (namely substituting for Ba) as in the case with $La_{2-x}(Ca,Sr,Ba)_xCuO_4$. However, by chemical substitution

in $BaCoS_2$ it is possible to produce a rich diversity of structural, magnetic, and electronic phases as a function of temperature and chemical composition. Substitution of Co by Ni produces a continuous change from the antiferromagnetic semiconducting phase to a paramagnetic metallic phase with the crossover in both the electrical and magnetic properties occurring near $x=0.25$ in the $BaCo_{1-x}Ni_xS_2$ $(0\leqslant x\leqslant 1)$ series.[1,7,11] Also Cu has been substituted for Co up to a concentration of $x\simeq 0.5$. Compounds in the $BaCo_{1-x}Cu_xS_2$ series are semiconducting but there is a rapid decrease in T_N with increasing Cu concentration with a crossover near $x=0.15$ to a spin glass phase.[22,23] In addition, the series $Ba_{1-x}K_xCoS_2$ $(x\leqslant 0.07)$ (Ref. 24) and $Ba_{1-x}Bi_xCoS_2$ $(x\leqslant 0.07)$ (Ref. 25) have been studied.

Interest in the $BaCo_{1-x}Ni_xS_{2-y}$ series where sulfur vacancies are introduced has arisen due to the insulator-metal transition near 200 K. Following the initial report[1] that presented magnetic susceptibility, electrical resistance, and some structural data, there have been additional studies to characterize this anomalous transition. These include Mössbauer and specific heat,[26] high pressure,[27,28] neutron powder diffraction,[29] far-infrared reflectivity,[30] and thermal transport studies.[31] Also a similar transition has since been seen in $Ba_{1-x}K_xCoS_2$.[24] Our motivation for doping with Se was an attempt to raise the transition temperature for possible applications. We had found that a significant amount of Se could be substituted for S in $BaCoS_2$ and that Se goes on the S sites in the BaS layers. Thus doping Se in compounds that exhibit the transition would be expected to raise the transition temperature since the transition temperature in these compounds is known to decrease with increasing pressure[27,28] and the larger Se expands the lattice. We found this to be the case, but we also found that vacancies are not required for the transition to occur. We have investigated the stoichiometric $BaCo_{0.9}Ni_{0.1}S_{2-y}Se_y$ series where we have found it easier to produce samples that yield reproducible structural, electrical, and magnetic properties that vary systematically with the Se composition. While it is interesting to find the transition in this new series, the most important result of this investigation is the characterization of the low-temperature crystal structure.

In this paper we report on the new Se-doped stoichiometric $BaCo_{0.9}Ni_{0.1}S_{2-y}Se_y$ compounds. In Sec. II we describe experimental procedures. We discuss in some detail the synthesis of these materials since the magnetic and electrical measurements are quite sensitive to small concentrations of other barium cobalt sulfides, in particular Ba_2CoS_3. Also proper thermal treatment of the samples during preparation is required for samples to exhibit the insulator-metal transition. In Sec. III we report on the crystal structures as characterized by single-crystal and powder x-ray diffraction (XRD) studies. dc magnetic susceptibility measurements are used to characterize the magnetic properties, while dc resistance measurements are used to examine the conduction properties.

II. EXPERIMENTAL PROCEDURES

A. Synthesis

Polycrystalline samples of $BaCo_{0.9}Ni_{0.1}S_{2-y}Se_y$ were prepared using conventional solid-state reaction techniques starting with powders of the binary sulfides and selenides, BaS, CoS (a mixture of Co_9S_8 and β-$CoS_{1.1}$), NiS, CoSe, and NiSe. Stoichiometric quantities of the reactants were mixed, pressed into pellets, and sealed in quartz tubing at a pressure less than 10^{-5} torr. The sealed tubes were heated to 300 °C at 5 °C/min and held for 5 h, raised to 900 °C at 10 °C/min and held for 16 h, and quenched in water. The samples were then ground, pressed, resealed, and heated rapidly to 900 °C where the sample was held for 24 h before being quenched.

It is known[5] that $BaCoS_2$ is a metastable compound that must be prepared above 850 °C and rapidly quenched to prevent decomposition into Ba_2CoS_3 and CoS upon cooling. Likewise, the quenching of the $BaCo_{0.9}Ni_{0.1}S_{2-y}Se_y$ samples is required to avoid multiphase samples with significant Ba_2CoS_3 contamination. Following this procedure we were able to prepare sintered single-phase samples of $BaCo_{0.9}Ni_{0.1}S_{2-y}Se_y$ for $y\leqslant 0.4$. The samples varied in color from black to dark gray with increasing Se content and contained very small platelike crystals.

Finally the samples were annealed in sealed quartz tubes at 540 °C for 5 h. As in the case of the previously studied sulfur-deficient compounds $BaCo_{0.9}Ni_{0.1}S_{2-y}$ $(0\leqslant y\leqslant 0.2)$, rapidly quenched samples do not undergo the insulator-to-metal transition with decreasing temperature unless they are annealed. The annealing parameters for the Se-doped samples were determined by trial and error. Samples annealed at temperatures above 550 °C for a few hours would contain significant amounts of Ba_2CoS_3, while samples annealed at temperatures below 525 °C for many hours would not exhibit the insulator-to-metal transition. The annealing presumably reduces pinning imperfections.

B. Experimental details

Powder XRD patterns were obtained at room temperature and 110 K for all the $BaCo_{0.9}Ni_{0.1}S_{2-y}Se_y$ samples. The data were collected with a Siemens D 5000 diffractometer using Cu $K\alpha$ radiation. These patterns were used to confirm the lattice structure, inspect for additional phases, and determine lattice constants. Also single crystals were extracted from the $BaCo_{0.9}Ni_{0.1}S_{1.8}Se_2$ sample and data collected on an Enraf-Nonius CAD4 four-circle diffractometer and also on a Bruker Smart 1000 charge-coupled device (CCD) system. The single-crystal diffraction measurements were used to determine the previously unknown crystal structure of the low-temperature metallic phase.

Magnetic susceptibility measurements were made in several applied fields between 1 and 50 kOe and at temperatures between 5 and 350 K using a Quantum Design superconducting quantum-interference device (SQUID) magnetometer. The susceptibilities of the samples in the series $BaCo_{0.9}Ni_{0.1}S_{2-y}Se_y$ showed no observable field dependence for this range of fields. Resistance measurements as a function of temperature were made on bars cleaved from the sintered polycrystalline pellets. The measurements were performed with a current of 1 mA using a standard four-wire configuration with copper wire contacts that were attached with silver epoxy. The current was reversed during each measurement.

III. EXPERIMENTAL RESULTS

A. Crystal structures

The layered compound $BaNiS_2$ has a tetragonal structure with $P4/nmm$ symmetry[32] where there are two formula units per unit cell. The dimension of this tetragonal cell perpendicular to the layers is approximately twice the parallel dimensions. In this structure the Ni sites are pentacoordinated to S sites in a square-pyramidal environment. These edge-sharing pyramids alternate above and below the plane that is formed by the basal-plane S(2) sulfur atoms. The Ni atoms and S(2) sulfur atoms form $(NiS_{4/4})_2$ sheets within which the Ni atoms are displaced above and below the S(2) plane. The apical S(1) sulfur atoms together with the Ba atoms form slightly distorted rocksalt layers between these Ni-S sheets.

The $BaCoS_2$ structure is distinguished from the $BaNiS_2$ structure by a slight monoclinic distortion where the angle between the axes of the formerly square lattice of the layers opens from 90° to 90.45(2)°. This structure has been refined in the monoclinic $P2/n$ space group.[4] Since this distortion leaves the two axes with equal lengths, there is a larger equivalent C-centered orthorhombic unit cell. The structure has also been refined in the orthorhombic $Cmma$ symmetry.[5] These two refinements yield essentially identical results for the structure and have similarly good estimates for the quality of the fit of the single-crystal x-ray data. Previous studies[11] of the $BaCo_{1-x}Ni_xS_2$ series have shown that this distortion in $BaCoS_2$ is rapidly suppressed by Ni substitution such that the compounds are tetragonal for $x \geq 0.1$.

The structure of the room-temperature semiconducting phase of the $BaCo_{0.9}Ni_{0.1}S_{2-y}Se_y$ compounds exhibits a monoclinic distortion relative to the tetragonal $BaCo_{0.9}Ni_{0.1}S_2$ structure that increases with increasing Se concentration. This distortion is the same as in $BaCoS_2$ except that it is smaller even at the largest Se doping possible ($y \sim 0.5$). Single-crystal XRD data for a $y=0.2$ sample were refined to a residual index $R_1=0.017$ in the $P2/n$ space group using the monoclinic primitive cell. The most interesting result from this refinement is that the Se substituted for S only on the S(1) sites, the sulfur sites in the BaS layers. This is probably a simple consequence of Se being too large to substitute on the S(2) sites of the $(Co_{0.9}Ni_{0.1})$-S sheets. The property that Se can substitute for S only in the BaS layers does not depend on whether the sample was annealed after quenching. Also we have seen exactly the same result with a $BaCoS_{0.8}Se_{0.2}$ crystal.

As in the case of $BaCoS_2$, the high-temperature $BaCo_{0.9}Ni_{0.1}S_{2-y}Se_y$ structure can be equally well described in the $Cmma$ space group using the larger C-centered orthorhombic cell. Since the low-temperature structure resulting from the phase transition requires a monoclinic primitive cell corresponding to a distortion of this orthorhombic cell, it is convenient to think of the high-temperature structure in terms of the orthorhombic description. Hence, in Fig. 1 we give the room-temperature lattice constants for the orthorhombic unit cell of $BaCo_{0.9}Ni_{0.1}S_{2-y}Se_y$ as a function of Se concentration $y \leq 0.5$ determined by powder XRD. As the Se concentration increases from $y=0$ to $y=0.4$, the lattice constants increase linearly. For $y \geq 0.5$, the powder diffraction patterns showed the presence of additional phases and the lattice constants were inconsistent with the linear increase

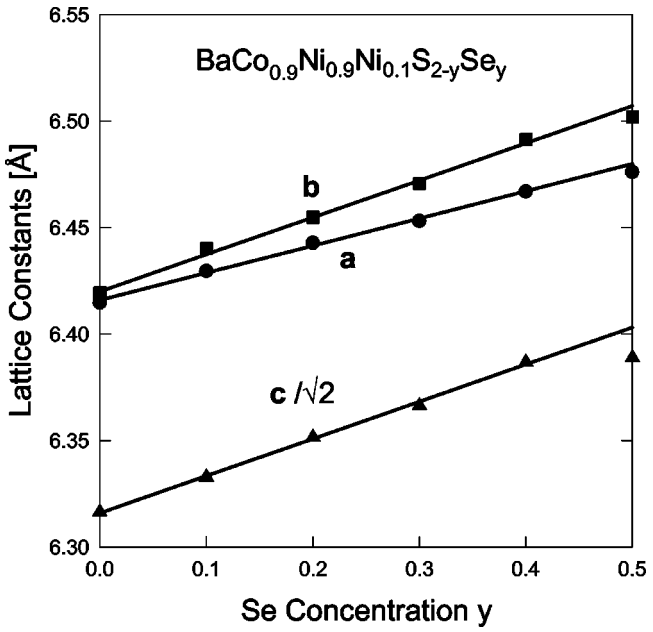

FIG. 1. Lattice constants of orthorhombic $BaCo_{0.9}Ni_{0.1}S_{2-y}Se_y$ as a function of Se concentration y at room temperature. Lines are linear fits to $y \leq 0.4$ measurements.

observed at lower concentrations. It thus appears that the maximum Se concentration is near $y=0.5$ where one-half of the S(1) sites would be occupied. From the structure and the lattice constants one can calculate interatomic distances. In the $y=0$ compound the Co-S(1) distances are 2.32 Å, the Co-S(2) are 2.39 Å, and the Co-Co distance is 3.55 Å. For $y=0.4$ these lengths are about 0.03 Å larger.

The antiferromagnetic-semiconductor to paramagnetic-metal transition that occurs at lower temperatures is associated with a radical structural change. From XRD studies at low temperatures on a number of single crystals in the sulfur-deficient series $BaCo_{1-x}Ni_xS_{2-y}$ and on $BaCo_{0.9}Ni_{0.1}S_{1.8}Se_2$ crystals, we have been able to obtain a fairly satisfactory picture of the crystal structure in the low-temperature metallic phase. This structure determination has been a very difficult problem requiring advanced analysis of data collected with an area detector. Full details will be presented elsewhere. Also some of the sulfur-deficient compounds studied earlier showed evidence for superstructures. However, the fundamental structure is a monoclinic structure that results from a shearlike displacement of the BaS layers of the high-temperature orthorhombic structure that produces a monoclinic angle of 98.98°. Although individual BaS layers are only slightly distorted, there is a major rearrangement of atoms in the Co-S sheets. The coordination of Co atoms with sulfur atoms changes from fivefold where the Co was centered in a square pyramid to a fourfold coordination where Co is now in a distorted tetrahedron. Furthermore, each Co atom shares its tetrahedron at the edges with that of a neighboring Co such that the Co-Co distance is only 2.6 Å as compared with the 3.6 Å Co-Co distance in high-temperature phase. These Co-dimer units then share vertices to form the Co-S layer. Since neighboring units are oriented differently, the primitive monoclinic cell contains four formula units. There is a 1.5% increase in volume associated with the transition, the volume being greater in the low-temperature phase.

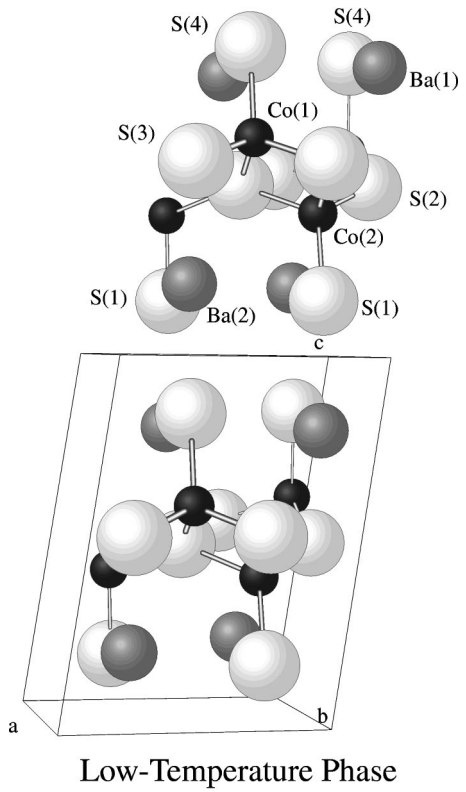

FIG. 2. Crystal structure of the low-temperature monoclinic phase of $BaCo_{0.9}Ni_{0.1}S_{2-y}Se_y$. Small dark spheres denote Co sites, intermediate spheres Ba sites, and large light spheres S sites.

The monoclinic structure determined for the low-temperature phase of the $BaCo_{0.9}Ni_{0.1}S_{2-y}Se_y$ compounds is shown in Fig. 2. The diagram is two unit cells high and oriented so as to show the displacement of the BaS layers and the resulting monoclinic angle. A clearer picture of the rearrangement that occurs in the Co-S sheets is given in Fig. 3, which shows the structure of the Co-S sheet for both the low- and high-temperature phases. The crystallographic parameters for the low-temperature phase of $BaCo_{0.9}Ni_{0.1}S_{1.8}Se_2$ refined in the monoclinic Pa space group are given in Table I. For each site listed there is a symmetry related site at $(x+\frac{1}{2},-y,z)$. This multiplicity of 2 compares with that of 4 for the Ba, Co, S(1), and S(2) sites of the orthorhombic $Cmma$ structure. In our notation the S(1) sites of the BaS layers in the orthorhombic structure are replaced by the S(1) and S(4) sites in the monoclinic structure with Pa symmetry, the S(1) sites being below the Co_2S_2 sheets and the S(4) sites above. Similarly S(2) sites in the Co_2S_2 sheets are replaced by slightly noncoplanar S(2) and S(3) sites. The four Co-S distances, calculated from the data in Table I, range from 2.19 to 2.27 Å and the Co(1)-Co(2) distance is 2.57 Å. The Co-S distances are significantly shorter than in the high-temperature phase where the Co atoms have a fivefold coordination with the sulfur atoms. These shorter distances are similar to the distances found in Co_3S_4 and Co_9S_8 for four coordinate Co. The Co(1)-Co(2) distance of 2.57 Å is similar to the 2.50 Å distance in Co metal. Finally, as seen from the results for the site occupation factors given in Table I, Se substitutes for S preferentially on the S(1) sites. This is consistent with the observation that $y=0.5$ seem to be the limit for the Se concentration.

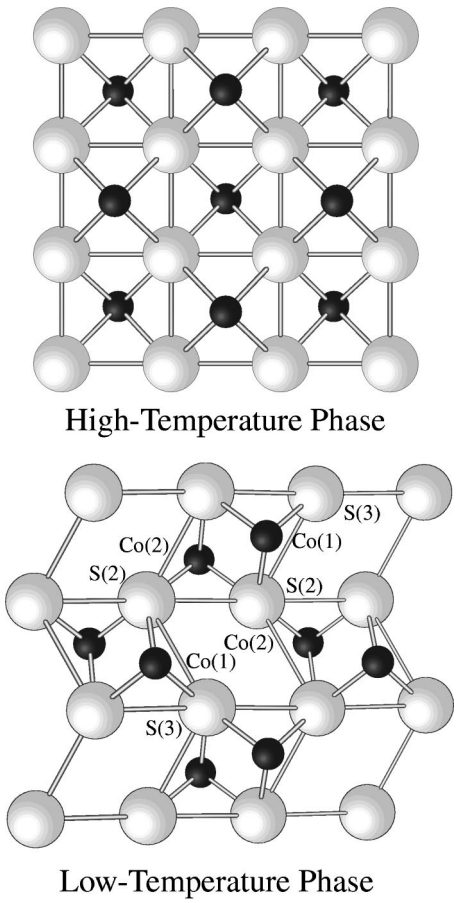

FIG. 3. Perpendicular view of the Co_2S_2 sheet of $BaCo_{0.9}Ni_{0.1}S_{2-y}Se_y$ for the low-temperature phase and the high-temperature phase. Small spheres denote Co sites, and large spheres S sites.

The result that the XRD data for the high-temperature phase could be refined in the $Cmma$ symmetry where S(1) and S(4) are equivalent might be explained by there being unresolved twins.

Powder XRD patterns were obtained for all the $BaCo_{0.9}Ni_{0.1}S_{2-y}Se_y$ samples at 110 K, which is well below the transition temperature. These patterns clearly show that a

TABLE I. Fractional atomic coordinates (x,y,z), equivalent isotropic displacement parameters $[U_{eq}$ (Å^2)], and site occupation factors (SOF) for $BaCo_{1.9}Ni_{0.1}S_{1.8}Se_{0.2}$ refined in the space group Pa to $R_1=0.07$. The lattice parameters are $a=6.618(5)$ Å, $b=6.382(7)$ Å, $c=9.094(9)$ Å, and $\beta=98.97(11)°$.

Atom	x	y	z	U_{eq}	SOF
Ba(1)	0.6612	0.2549	0.7990	0.015	1
Ba(2)	0.2515	0.2452	0.1972	0.015	1
Co(1)	0.1067	0.1968	0.5960	0.022	1
Co(2)	0.7997	0.2904	0.3975	0.014	1
S(1)	0.7330	0.2508	0.1460	0.017	0.74
Se(1)	0.7330	0.2508	0.1460	0.017	0.26
S(2)	0.0730	0.5044	0.4785	0.013	1
S(3)	0.8438	0.9974	0.5207	0.019	1
S(4)	0.1670	0.2466	0.8449	0.020	0.92
Se(4)	0.1670	0.2466	0.8449	0.020	0.08

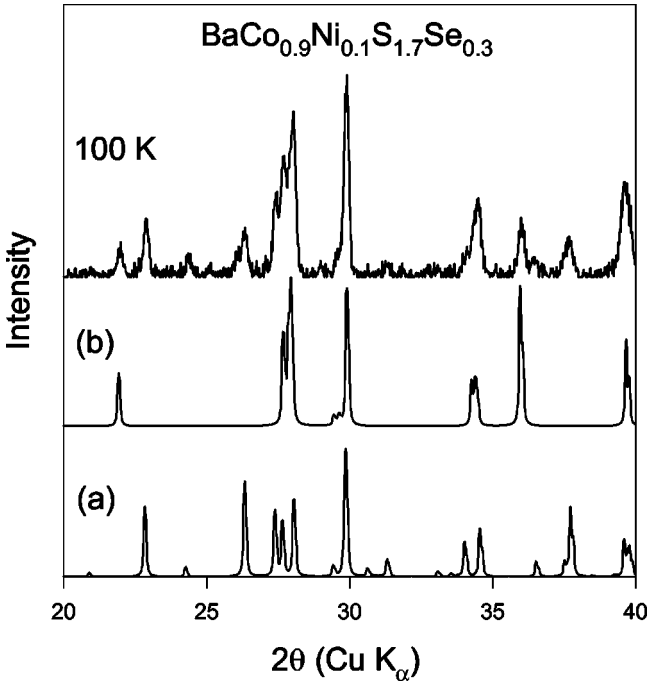

FIG. 4. X-ray powder diffraction pattern of $BaCo_{0.9}Ni_{0.1}S_{1.7}Se_{0.3}$ at 110 K with background subtracted, and calculated patterns for (a) the low-temperature phase and (b) the high-temperature phase.

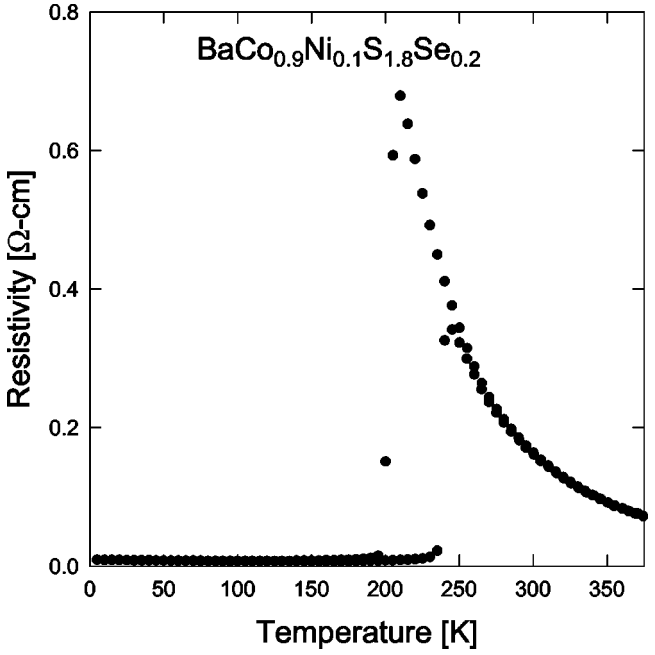

FIG. 5. The electrical resistance for $BaCo_{0.9}Ni_{0.1}S_{1.8}Se_{0.2}$ as a function of temperature on warming and cooling.

significant fraction of the material remains in the high-temperature phase as we had previously seen in the case of the sulfur-deficient $BaCo_{1-x}Ni_xS_{2-y}$ compounds. We have not attempted to investigate how this fraction might depend on the annealing temperatures and times used in preparing the samples, or on the grinding to produce powders from the sintered samples. Our main motivation for the low-temperature powder studies was to confirm that the structure determined for the single crystals is the unique structure for the low-temperature phase of the $BaCo_{0.9}Ni_{0.1}S_{2-y}Se_y$ compounds. The XRD pattern for the $y=0.3$ sample at 110 K with background subtracted is shown in Fig. 4. We find that the pattern calculated for a 55:45 mixture of the low- and high-temperature phases yields a good fit of the measured pattern. The powder patterns calculated for the low- and high-temperature structures are shown separately in the lower part of the figure for comparison with the measured pattern. These calculated patterns include a simple correction for a preferred orientation since the crystals of these materials are platelets which orient when the powders are pressed into the holders. For the other samples where $0.1 \leqslant y \leqslant 0.4$, we find similar results. The percentage of low-temperature phase material was variable but in the range from 50% to 60%. However, for $y=0.0$ the powder XRD pattern at 110 K shows additional features. It appears that without the Se doping several related low-temperature structures are possible as has been indicated by our earlier work on the sulfur-deficient $BaCo_{1-x}Ni_xS_{2-y}$ compounds.

B. Resistance and magnetic susceptibility

The electrical resistivities measured for sintered polycrystalline bars of $BaCo_{0.9}Ni_{0.1}S_{2-y}Se_y$ with $y \leqslant 0.4$ do not depend strongly on the Se concentration. Since one expects charge transport to be mostly confined to the Co-S sheets, this observation is consistent with the structural result that shows Se confined to the BaS layers. The temperature dependence is essentially the same as seen in the sulfur-deficient $BaCo_{0.9}Ni_{0.1}S_{2-y}$ $(0.05 \leqslant y \leqslant 0.20)$ series as previously reported;[1] namely, there is an approximate $\rho = \rho_0 \exp(\Delta/k_BT)$ behavior at high temperature, a hysteretic transition, and a significantly smaller resistivity at low temperatures that is nearly temperature independent. The electrical resistivity for $BaCo_{0.9}Ni_{0.1}S_{1.8}Se_{0.2}$ is shown in Fig. 5. The sample was initially cooled to 5 K, and resistance measurements were made as the sample warmed to 375 K and then cooled back to 5 K. Resistivities for these sintered polycrystalline samples were estimated from the resistance measurements with no correction for porosity or intergrain effects. A fit of the resistivity above 325 K to the exponential behavior gives $\Delta = 0.11$ eV. In the series the values for Δ fall between 0.07 and 0.11 eV, there being an initial increase in Δ with increasing Se concentration followed by a decrease. It is unlikely that this activation energy is attributable to an intrinsic band gap, since we have seen significant variation in Δ for samples of the same nominal composition that were prepared with different reactants or were quenched and annealed differently. The drop in resistivity at the insulator-to-metal transition is in the range of two orders of magnitude. For the series we find that the low-temperature resistivities decrease with increasing Se doping from 10^{-2} to 3×10^{-3} Ω cm. However, since the samples are quite porous and the powder XRD studies show that only some fraction of a sample undergoes the transition, the resistivity of the low-temperature phase in the plane of the Co-S sheets is probably much smaller. Thus the data support the interpretation of the low-temperature phase as a poor metal with a resistivity similar to that of $BaNiS_2$. Finally the transition temperature increases with increasing Se concentration, being approximately 25% higher in the $y=0.4$ compound than in the undoped compound.

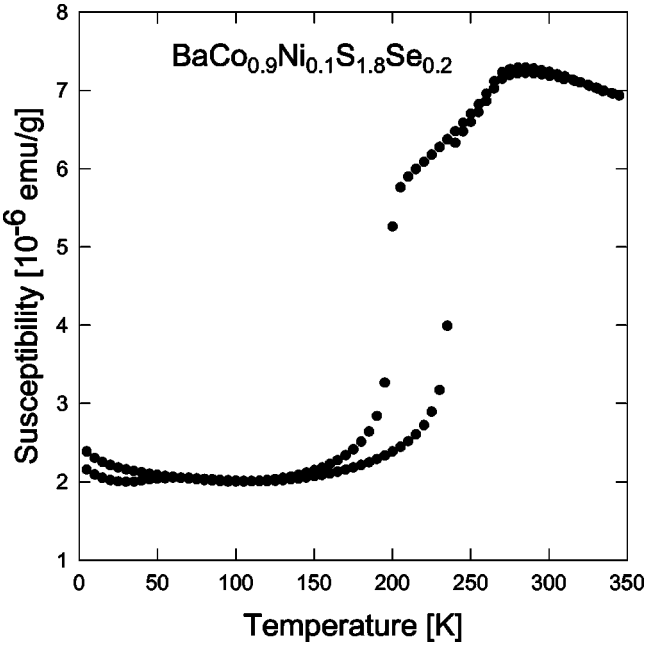

FIG. 6. The magnetic susceptibility for $BaCo_{0.9}Ni_{0.1}S_{1.8}Se_{0.2}$ as a function of temperature where the sample was first cooled in zero field, a field of 1.0 kOe applied, and measurements made as the sample was warmed and then cooled.

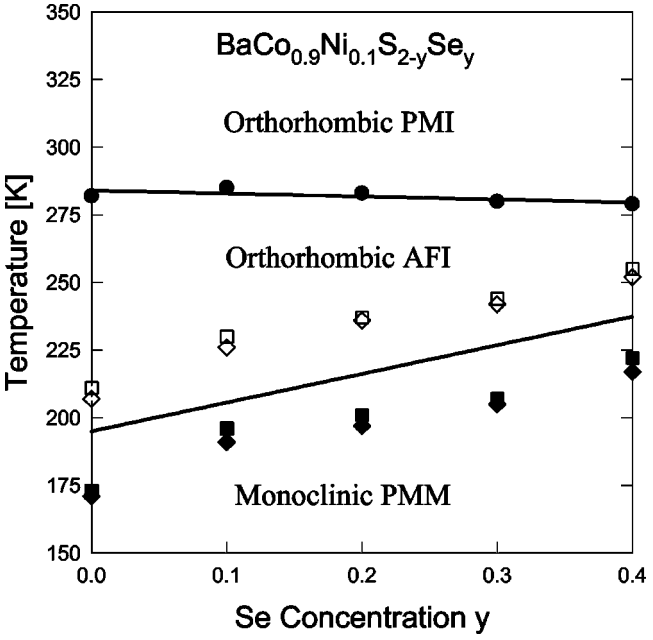

FIG. 7. Phase diagram for $BaCo_{0.9}Ni_{0.1}S_{2-y}Se_y$. The different phases are paramagnetic insulator (PMI), antiferromagnetic insulator (AFI), and paramagnetic metal (PMM). The Néel temperatures for PMI-AFI transitions are denoted by the solid circles, and the transition temperatures for AFI-PMM are denoted by squares and diamonds as determined from resistance and magnetic susceptibility, respectively; solid and open symbols for cooling and warming, respectively. The lines are estimates for the phase boundaries based on linear fits to the transition temperatures.

The temperature dependence of the magnetic susceptibility for $BaCo_{0.9}Ni_{0.1}S_{1.8}Se_{0.2}$ is shown in Fig. 6. The data presented is for a zero-field-cooled/field-cooled (ZFC/FC) set of measurements, i.e., first the sample was cooled to 5 K in zero magnetic field; then a field of 1.0 kOe was applied and measurements taken as the sample was warmed to 350 K and cooled back to 5 K. The behavior of the susceptibility is the same as previously reported[1] for the sulfur-deficient $BaCo_{0.9}Ni_{0.1}S_{2-y}$ $(0.05 \leqslant y \leqslant 0.20)$ series; namely, Curie-Weiss behavior at high temperature, a broad maximum associated with a second-order transition to antiferromagnetic order, and at lower temperatures a first-order transition to predominantly Pauli paramagnetic behavior. Using the temperature where the susceptibility is a maximum as an estimate of the Néel temperature T_N we find $T_N \simeq 280$ K as compared with 310 K for $BaCoS_2$ where antiferromagnetic ordering has been clearly identified by neutron diffraction studies.[12,13] The lower value for T_N is fully attributable to the Ni concentration being 0.1 as shown by the dependence of T_N on Ni concentration found in the $BaCo_{1-x}Ni_xS_2$ series.[11] For the $BaCo_{0.9}Ni_{0.1}S_{2-y}Se_y$ series with $y \leqslant 0.4$, the measured susceptibilities showed no systematic dependence on the Se concentration except for an increase in the insulator-metal transition temperature with Se concentration. Again this is consistent with our finding that Se substitutes for S only in the BaS layers. In contrast, in the $BaCo_{0.9}Ni_{0.1}S_{2-y}$ $(0.05 \leqslant y \leqslant 0.20)$ series T_N increases with increasing S deficiency.

For all the samples the susceptibility below the insulator-metal transition is of the order of 2×10^{-6} emu/g as compared with low-temperature susceptibilities of 2×10^{-7} emu/g for the paramagnetic metal $BaNiS_2$ and 5×10^{-6} emu/g for antiferromagnetic semiconductor $BaCoS_2$ (or $BaCo_{0.9}Ni_{0.1}S_{2-y}$ samples that have not been annealed and therefore do not exhibit the transition). Since only some fraction of the material undergoes the transition, it is likely that the true susceptibility of the low-temperature phase is much smaller than the 2×10^{-6} emu/g. Thus the susceptibility of the low-temperature phase is consistent with a paramagnetic metal similar to $BaNiS_2$. Below 50 K irreversibility is seen in the ZFC/FC data that is not seen if the magnetic field is applied before cooling. This could indicate a small amount of a ferromagnetic phase or a spin-glass phase. Also there is an increase with decreasing temperature at lower temperatures that is likely associated with dilute concentration of magnetic impurity ions. From an analysis of measurements below 5 K and in fields up to 50 kOe we estimate the magnetic impurity concentration to be of the order of 100 to 500 ppm, which is reasonable for the purity of the starting materials.

From the resistivity and magnetic susceptibility data one can construct a phase diagram for $BaCo_{0.9}Ni_{0.1}S_{2-y}Se_y$. The result is shown in Fig. 7. The boundary between paramagnetic insulator (PMI) and antiferromagnetic insulator (AFI) is determined by the temperature of the peak in the susceptibility although this transition can also be seen in the resistivity as a less well-defined local maximum in the logarithmic derivative of the resistance. Owing to the hysteresis in the first-order antiferromagnetic-insulator–paramagnetic-metal (AFI-PPM) transition, transition temperatures are indicated for both warming and cooling. The actual values are determined from the midpoints of the nearly discontinuous transitions in both the resistivities and magnetic susceptibilities. The width of the hysteresis is essentially independent of

the Se concentration and equal to about 35 K. The AFI-PMM boundary drawn is a straight-line fit of the averages for warming and cooling.

This phase diagram for $BaCo_{0.9}Ni_{0.1}S_{2-y}Se_y$ as a function of Se concentration can be compared with the previously published[27] diagram for $BaCo_{0.9}Ni_{0.1}S_{1.9}$ as a function of pressure. In that case the AFI-PMM transition temperature decreased with increasing hydrostatic pressure such that $dT/dp \simeq -240$ K/GPa, and T_N was nearly independent of pressure for $p \lesssim 0.2$ GPa. In the present case of the Se-doped compounds T_N is nearly independent of the Se concentration and $dT/dy \simeq 100$ K for the slope of the AFI-PMM coexistence curve. Thus the effect of doping with Se is essentially equivalent to an increasing negative pressure. This is consistent with the Se ion being significantly larger than the S ion and the observation that Se substitutes for S only in the BaS layers.

IV. DISCUSSION

Knowledge of the structure of the low-temperature phase is certainly a prerequisite for understanding this unusual insulator-to-metal transition that has been found to occur for certain ranges of composition in $BaCo_{1-x}Ni_xS_{2-y}$, $Ba_{1-x}K_xCoS_2$, and now also $BaCo_{1-x}Ni_xS_{2-y}Se_y$. Although we have been able to fully characterize the structure only in the case of the Se doped series, it is clear from our previous work on the sulfur-deficient series that the displaced BaS layers, the Co dimers, and the fourfold coordination of each Co atom with its sulfur neighbors, are common structural features of the low-temperature phase in all these materials. Since the BaS layers are only slightly distorted, it is reasonable to try to explain the required lower energy for this phase in terms of the rearrangement of the atoms in the Co-S sheets. In support of this view is the observation that the type of square lattice of $CoS_{4/4}$ units that characterizes the sheets in the high-temperature phase is exceptional for layered late transition-metal sulfides. In the case of Co the only examples are $BaCoS_2$ and $TlCo_2S_2$. Now that the low-temperature structure is known it might be possible to calculate electronic properties for a quantitative understanding.

Although we use the term paramagnetic metal for the low-temperature phase, the physics is probably much more exotic than this term implies. Far-infrared studies in $BaCo_{0.9}Ni_{0.1}S_{1.9}$ indicated an anomalous metallic state with a very small ratio of carrier density to effective mass ($n m_e/m^* \sim 10^{18}$ cm^{-3}).[30] The metallic behavior is possibly associated with a small concentration of charge carrying excitations relative to the quasi-2D lattice of valence-bonded Co dimers. Also in this picture the magnetic transition is from an antiferromagnetic state to a valence-bond state. In the antiferromagnetic state, as characterized by neutron diffraction studies,[12,13,29] the Co above and below the S plane each form two-dimensional antiferromagnetic lattices. Since the coupling between nearest-neighbor Co sites is frustrated, the dimer (valence-bond) state could certainly have the lower energy in this localized electron picture.

On a qualitative level the more puzzling problem is the required higher entropy of the antiferromagnetic semiconducting phase relative to the paramagnetic metallic phase. Based on the pressure studies,[27] the entropy change at this first-order transition was estimated to be 0.6 ± 0.2 cal/mol K (note that $N_A k_B \ln 2 = 1.4$ cal/mol K). Since it is unlikely that electronic or magnetic contributions to the entropy are greater in the high-temperature phase, the higher entropy is probably associated with a greater lattice contribution.

ACKNOWLEDGMENTS

This work was supported in part by National Science Foundation Grants No. DMR-93-18333 and DMR-93-18385, a Carver Scientific Research Initiative Grant.

*Present address: Secure Computing Corporation, Roseville, Minnesota 55113.

[1] L. S. Martinson, J. W. Schweitzer, and N. C. Baenziger, Phys. Rev. Lett. **71**, 125 (1993).

[2] L. F. Mattheiss, Solid State Commun. **93**, 879 (1995).

[3] I. Hase, N. Shirakawa, and Y. Nishihara, J. Phys. Soc. Jpn. **64**, 2533 (1995).

[4] N. C. Baenziger, L. Grout, L. S. Martinson, and J. W. Schweitzer, Acta Crystallogr., Sect. C: Cryst. Struct. Commun. **50**, 1375 (1994).

[5] G. J. Snyder, M. C. Gelabert, and F. J. DiSalvo, J. Solid State Chem. **113**, 355 (1994); M. C. Gelabert, N. E. Brese, F. J. DiSalvo, S. Jobic, P. Deniard, and R. Brec, *ibid.* **127**, 211 (1996).

[6] K. Kodama, H. Fujishita, H. Harashina, S. Taniguchi, J. Takeda, and M. Sato, J. Phys. Soc. Jpn. **64**, 2069 (1995).

[7] J. Takeda, K. Kodama, H. Harashina, and M. Sato, J. Phys. Soc. Jpn. **63**, 3564 (1994).

[8] J. Takeda, Y. Kobayashi, K. Kodama, H. Harashina, and M. Sato, J. Phys. Soc. Jpn. **64**, 2550 (1995).

[9] K. Kodama, S. Shamoto, H. Harashina, J. Takeda, M. Sato, K. Kakurai, and M. Nishi, J. Phys. Soc. Jpn. **65**, 1782 (1996).

[10] Y. Yasui, Y. Kobayashi, J. Takeda, S. Shamoto, and M. Sato, J. Phys. Soc. Jpn. **65**, 2757 (1996).

[11] L. S. Martinson, J. W. Schweitzer, and N. C. Baenziger, Phys. Rev. B **54**, 11 265 (1996).

[12] S. Shamoto, K. Kodama, H. Harashina, M. Sato, and K. Kakurai, J. Phys. Soc. Jpn. **66**, 1138 (1997).

[13] D. Mandrus, J. L. Sarrao, B. C. Chakoumakos, J. A. FernandezBaca, S. E. Nagler, and B. C. Sales, J. Appl. Phys. **81**, 4620 (1997).

[14] J. Takeda, Y. Yasui, H. Sasaki, and M. Sato, J. Phys. Soc. Jpn. **66**, 1718 (1997).

[15] Y. Yasui, H. Sasaki, S. Shamoto, and M. Sato, J. Phys. Soc. Jpn. **66**, 3194 (1997).

[16] H. Sasaki, H. Harashina, K. Kodama, S. Shamoto, M. Sato, K. Kakurai, and M. Nishi, J. Phys. Soc. Jpn. **66**, 3975 (1997); H. Sasaki, H. Harashina, K. Kodama, M. Sato, S. Shamoto, M. Nishi, and K. Kakurai, *ibid.* **67**, 4235 (1998).

[17] E. Z. Kurmaev, S. Bartkowski, M. Neumann, S. Stadler, D. L. Ederer, V. R. Galakhov, Y. M. Yarmoshenko, I. V. Solovyev, S. N. Shamin, V. A. Trofimova, and D. A. Zatsepin, J. Electron Sepctrosc. Relat. Phenom. **88**, 441 (1998); E. Z. Kurmaev, Y. M. Yarmoshenko, M. Neumann, S. Stadler, D. L. Ederer, I. Hase, A. Fujimori, M. Sato, Y. Yasui, R. C. C. Perera, M. M.

Grush, T. A. Callcott, D. A. Zatsepin, V. A. Trofimova, and V. V. Sokolov, J. Phys. Chem. Solids **59**, 1459 (1998).
[18] B. Fisher, J. Genossar, L. Patlagan, G. M. Reisner, and A. Knizhnik, Physica B **261**, 855 (1999); Phys. Rev. B **59**, 8747 (1999).
[19] Y. Yasui, H. Sasaki, M. Sato, M. Ohashi, Y. Sekine, C. Murayama, and N. Mori, J. Phys. Soc. Jpn. **68**, 1313 (1999).
[20] T. Takeda, J. Sakurai, A. Nakamura, M. Kato, Y. Kobayashi, and M. Sato, J. Phys. Soc. Jpn. **68**, 1602 (1999).
[21] M. Kanada, H. Harashina, H. Sasaki, K. Kodama, M. Sato, K. Kakurai, M. Nishi, E. Nishibori, M. Sakata, M. Takata, and T. Adachi, J. Phys. Chem. Solids **60**, 1181 (1999).
[22] W. J. Zhu, S. T. Ting, H. H. Feng, and P. H. Hor, J. Solid State Chem. **138**, 111 (1998).
[23] L. S. Martinson, J. W. Schweitzer, and P. M. Shand (unpublished).
[24] M. C. Gelabert, R. J. Lachicotte, and F. J. DiSalvo, J. Chem. Mater. **10**, 613 (1998).
[25] A. Irizawa, K. Yoshimura, K. Kosuge, C. Dusek, H. Michor, and G. Hilscher, J. Phys. Soc. Jpn. **68**, 3016 (1999).
[26] I. Felner, J. Gersten, S. Litvin, U. Asaf, and T. Kröner, Phys. Rev. B **52**, 10 097 (1995).
[27] C. Looney, J. S. Schilling, L. S. Martinson, and J. W. Schweitzer, Phys. Rev. Lett. **76**, 4789 (1996).
[28] H. Kang, I. V. Medvedeva, K. Barner, and U. Sondermann, Physica B **245**, 20 (1998).
[29] S. A. M. Mentink, T. E. Mason, B. Fisher, J. Genossar, L. Patlagan, A. Kanigel, M. D. Lumsden, and B. D. Gaulin, Phys. Rev. B **55**, 12 375 (1997).
[30] K. H. Kim, Y. H. Kim, L. S. Martinson, and J. W. Schweitzer, Phys. Rev. Lett. **78**, 4498 (1997).
[31] H. Kang, P. Mandal, I. V. Medvedeva, K. Barner, A. Poddar, and E. Gmelin, Phys. Status Solidi A **163**, 465 (1997); H. Kang, P. Mandal, I. V. Medvedeva, J. Liebe, G. H. Rao, K. Barner, A. Poddar, and E. Gmelin, J. Appl. Phys. **83**, 6977 (1998).
[32] I. E. Grey and H. Steinfink, J. Am. Chem. Soc. **92**, 5093 (1970); J. T. Maynard, E. I. du Pont de Nemours and Company, U.S. Patent No. 2,770,528, Nov. 1956.